Journal of Power Sources 211 (2012) 33–39

Contents lists available at SciVerse ScienceDirect

Journal of Power Sources

journal homepage: www.elsevier.com/locate/jpowsour

Facile hydrogen generation using colloidal carbon supported cobalt to catalyze hydrolysis of sodium borohydride

Jie Zhu, Rong Li, Weiling Niu, Yanjun Wu, Xinglong Gou*

Chemical Synthesis and Pollution Control Key Laboratory of Sichuan Province, College of Chemistry and Chemical Engineering, China West Normal University, Nanchong 637000, People's Republic of China

ARTICLE INFO

Article history:
Received 31 January 2012
Received in revised form
24 March 2012
Accepted 26 March 2012
Available online 13 April 2012

Keywords:
Sodium borohydride
Hydrolysis
Hydrogen generation
Cobalt catalysts
Colloidal carbon spheres

ABSTRACT

Colloidal carbon spheres (CCS) obtained from hydrothermal treatment of glucose are employed for the first time as a support for cobalt catalysts (CCS/Co) prepared by impregnation-chemical reduction method. Ultra-fine, almost amorphous cobalt metals bind tightly to the CCS surface and are distributed uniformly, creating highly-dispersed active sites which lead to facile catalysis of the hydrolysis of sodium borohydride in aqueous alkaline solution and rapid generation of hydrogen. An average hydrogen generation rate of 7.5, 8.4 and 10.4 L $min^{-1} \cdot g_{met}^{-1}$ is achieved at 20 °C for the CCS/Co catalysts with a Co loading content of 14.00, 15.45 and 18.38 wt%, respectively. The activation energy and enthalpy of the CCS/Co catalyzed $NaBH_4$ hydrolysis are found to be 24.04 and 21.51 kJ mol^{-1}, respectively. The low activation energy and rapid hydrogen generation rate suggest that the CCS-support Co materials are excellent catalysts for hydrogen production from borohydride hydrolysis.

1. Introduction

Public concerns about the depletion of fossil fuels and the problems associated with global warming and environmental pollution make the establishment of a clean and sustainable energy system a compelling need [1–3]. As an alternative fuel, hydrogen is considered as a promising clean energy carrier in future energy system with high energy density and zero emission [4,5]. However, hydrogen storage and production are major challenges to the widespread implementation of the hydrogen fuel cell technologies, especially for on-board automotive applications [6–9].

The potential utilization of $NaBH_4$ as a hydrogen storage material and as a fuel of direct fuel cell have been intensively investigated over the past decade thanks to its high hydrogen storage capacity of 10.8 wt%, commercial availability with low cost, high stability of its alkaline solutions, non-toxicity and fire-safety in comparison to many other hydrides [10–13]. Catalytic hydrolysis of $NaBH_4$ alkaline aqueous solution has been regarded as a promising and commercially feasible way to produce hydrogen for a proton exchange membrane fuel cell (PEMFC) and portable applications [14–17]. Active and stable catalysts for borohydride hydrolysis are one important consideration for generating the hydrogen needed for a practical fuel cell power-source system.

Up to now, a variety of catalysts including Lewis acids, precious metals, non-noble metals and some alloys, have been developed for catalytic hydrolysis of $NaBH_4$ [18–21]. Overall, precious metals exhibit better catalytic performance than non-noble metals. However, the high price of noble metals limits their large scale application. From the reactivity and cost point of view, cobalt-based catalysts are very efficient and have already proven to be a potential alternative to noble metals [22]. To reduce aggregation of the catalyst particles and further improve the catalytic activity, various materials such as carbon, oxides, hydroxyapatite, clay, heteropolyanions, polymer/hydrogel, and Ni foam have been chosen as the supports [23–29]. For example, the hydrogen generation rate attained with carbon supported Co-B film catalyst (8.1 L min^{-1} g_{cat}^{-1}) is significantly higher as compared to unsupported Co-B film (~4.33 L min^{-1} g_{cat}^{-1}) [30]. In terms of the self-weight and specific surface area, carbon materials have some advantages over many other supports, but their hydrophobic surface chemistry may weaken their affinity to Co nanoparticles as well as the contact with the $NaBH_4$ solution. Although some oxides with hydrophility such as Al_2O_3 and SiO_2 supported Co-based catalysts indeed show enhanced catalytic performance [31], they may suffer from corrosion in alkaline media, simultaneously increase burden by their self-weight on the hydrogen generation system.

Can we find a suitable support combining both advantages of favorable surface chemistry and light weight to improve the

* Corresponding author. Tel./fax: +86 817 256 8081.
E-mail address: gouxlr@126.com (X. Gou).

0378-7753/$ – see front matter © 2012 Elsevier B.V. All rights reserved.
doi:10.1016/j.jpowsour.2012.03.051

catalytic hydrogen generation activity of the supported cobalt catalysts? Inspired by this idea, we demonstrated in this work for the first time that the colloidal carbon spheres (CCS) obtained by hydrothermal treatment of glucose can be used as an idea substrate to support cobalt catalysts, and the as-prepared CCS-supported Co catalysts exhibited very high hydrogen generation rate (10.4 L min^{-1} g_{met}^{-1}) and exceptionally low activation energy (24.04 kJ mol^{-1}).

2. Experimental

2.1. Preparation of the CCS-supported Co catalysts

The CCS-supported Co catalysts were prepared by a two-step procedure. At the first stage, colloidal carbon spheres (CCS) were synthesized by hydrothermal treatment of glucose according to a previous reported method [32]. Typically, 80 mL of glucose solution with a concentration of 0.6 mol·L^{-1} was sealed in a Teflon-lined autoclave and maintained at 180 °C for 10 h. After reaction, the puce precipitate was separated by centrifugation, washed with de-ionized water and ethanol, and finally dried overnight at 60 °C in vacuum.

At the second stage, the CCS-supported Co catalysts were synthesized by the impregnation-chemical reduction method. In a typical synthesis, the required amount of CCS was dispersed into 40 mL cobalt acetate solution with the help of ultrasonic vibration. Subsequently, the mixture was stirred vigorously for one day to ensure sufficient adsorption of Co^{2+} on the surface of CCS. Then, an appropriate amount of fresh-prepared $NaBH_4$ aqueous solution was dropped slowly into the mixture, which was kept in a thermostatic bath with a temperature of 16 °C. After complete reduction of the Co^{2+}, the black precipitate was collected by centrifugation, washed thoroughly with distilled water and ethanol to remove residual ions, and finally dried at 60 °C in vacuum for 12 h to obtain the CCS-supported Co catalysts.

The Co loading on the as-prepared CCS-supported Co catalysts was tuned by varying the initial ratio of Co^{2+} and CCS. Unsupported Co catalysts were also produced via the same procedure in the absence of CCS. To investigate the effect of the heat treatment on the catalytic performance of the CCS-supported Co catalysts, factional CCS-supported Co catalysts were calcined in a tubular furnace under nitrogen atmosphere at 673 K for 2 h.

2.2. Characterization of the catalysts

The chemical composition and phase purity of the CCS-supported Co catalysts were determined by X-ray diffraction (XRD, Rigaku Ultima IV, Cu Kα radiation). The morphology of the catalysts was observed by using a scanning electron microscope (SEM, JEOL JSM-6510LV). The Co loading and elemental distribution of the catalysts were characterized by energy-dispersive X-ray spectroscopy (EDX, Oxford instruments X-Max). The specific surface area of the sample was measured by Brunauer-Emmett-Teller (BET) nitrogen adsorption-desorption (Belsorp-Mini II, BEL Japan, Inc.), and the pore size distribution was calculated by Barrett-Joyner-Halenda (BJH) formula.

2.3. Performance measurements of the catalysts

A certain amount of solid $NaBH_4$ and CCS-supported Co catalysts were first loaded into a round-bottom flask, which was immersed in a thermostatic bath to keep the temperature constant. Then, 10 mL of de-ionized water was introduced to initialize the hydrolysis of $NaBH_4$ under stirring. The generated hydrogen was led to a suction flask, which was pre-loaded with large mount of water and was connected to a graduated cylinder. The volume of hydrogen generated at a given interval was measured through a classic water-displacement method by reading the volume of the drained water in the cylinder. The hydrogen generation rate (HGR) was defined as $L \cdot min^{-1} \cdot g_{met}^{-1}$. For comparison the as-prepared CCS, CCS-supported Co catalysts with different cobalt loading, unsupported Co catalysts, and the calcined CCS-supported Co catalysts were also tested.

3. Results and discussion

3.1. Morphology and composition of the catalysts

As illustrated in Fig. 1, the colloidal carbon spheres (CCS) obtained from hydrothermal treatment of glucose were used as a support for preparation of the CCS-supported Co catalysts (CCS/Co) by an impregnation-reduction method. First, carbon spheres with a diameter of about 300 nm were synthesized from glucose under hydrothermal condition, and the sphere-like morphology was confirmed by SEM analysis as shown in Fig. 2 (a). BET measurements shows that the CCS sample possesses a porous structure with an average pore diameter of 5.7 nm, and has a high specific surface area of 20.071 m^2 g^{-1}, which is very beneficial to be used as a catalyst support. It is well known that the surface of the CCS from hydrothermal treatment of glucose bears lots of hydrophilic oxygen-containing groups such as −OH, and −COOH [32]. Therefore, the CCS support can be easily dispersed into aqueous cobalt acetate solution with the help of ultrasonic agitation. Meanwhile, Co^{2+} ions adsorbed tightly onto the surface of CCS through electrostatic/coordination interaction. Upon addition of $NaBH_4$ solution, Co^{2+} ions were readily *in-situ* reduced to cobalt metals, which uniformly deposited on the surface of the CCS support as depicted in Fig. 1.

From the SEM image shown in Fig. 2 (b) one can see that the morphology of the CCS-supported Co catalysts is very similar to the CCS, and there are no significant differences in the size of the spheres, indicating the Co layer deposited on the surface of the CCS was uniform and thin. The elemental composition and distribution were further analyzed by EDX, and the results are displayed in Fig. 2 (d)–(f). As expected, the CSS-supported catalysts were composed of C, Co and O, and the elemental distribution is very uniform. The average Co loading content in the CCS-supported Co catalysts was determined to be 14.00 wt%. A large amount of oxygen (37.72 wt%)

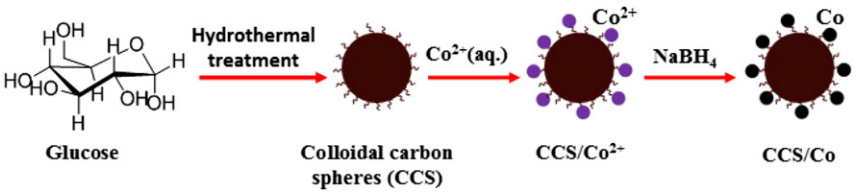

Fig. 1. Schematic representation of the preparation of the colloidal carbon spheres (CCS)-supported cobalt catalysts.

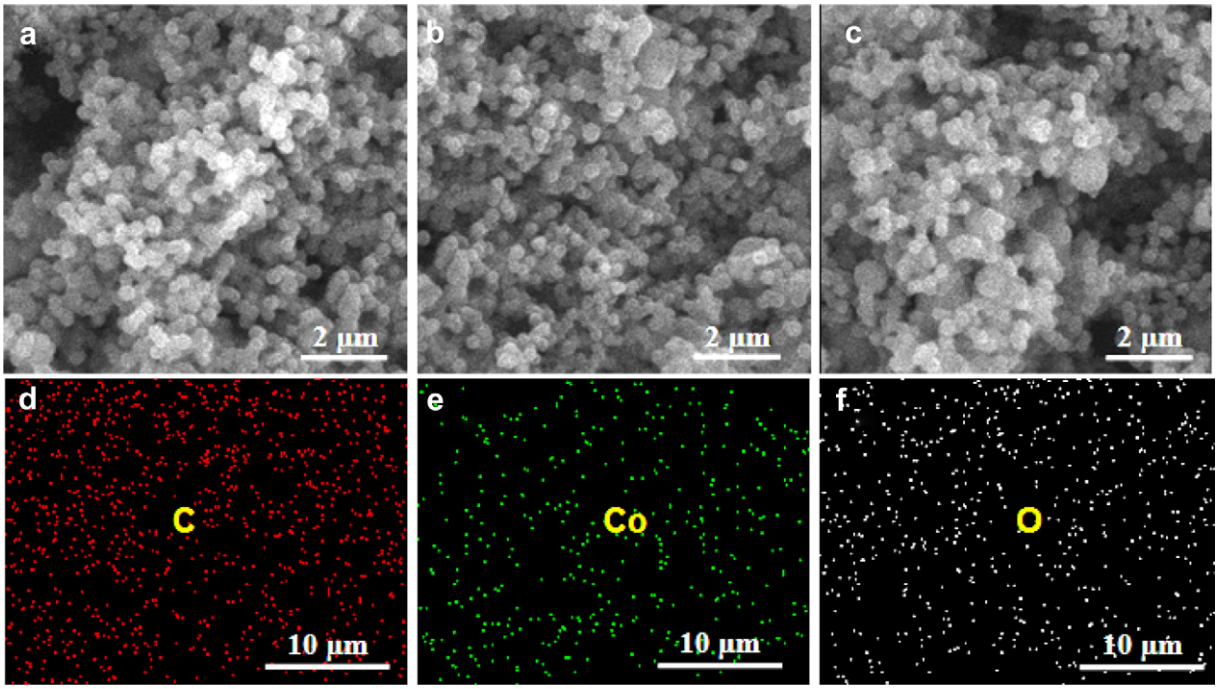

Fig. 2. SEM images of the as-prepared CCS (a), CCS-supported Co catalysts with different Co loading (b–c), and the elemental composition and distribution (d–f) of the CCS/Co sample shown in (b).

were also detected in the sample. Possibly, the element oxygen should be originated from the oxygen-containing groups on the surface of the CCS and the partial oxidation of the cobalt deposited on the support.

By controlling the initial ratio of CCS to Co^{2+} we can prepare CCS-supported Co catalysts with different Co loadings such as 15.45 wt% and 18.38 wt%. The morphology and size of all the supported catalysts resemble the CCS support. A typical SEM image of the CCS-supported catalysts with a Co loading of 18.38 wt% is shown in Fig. 2 (c), indicating the feasibility and generality of the method for preparation of CCS-supported catalysts. Note that element boron was not detected by EDX analysis for all of the as-prepared CCS-supported Co catalysts in our work, although most of the literature reported that Co_2B formed upon mixing the Co^{2+} solution and $NaBH_4$ through the reaction expressed in Equation (1) [33].

$$2Co^{2+} + 4BH_4^- + 9H_2O \rightarrow Co_2B + 12.5H_2 + 3B(OH)_3 \quad (1)$$

A previous report pointed out that ultra-fine, almost amorphous cobalt borides can be formed only under anaerobic conditions. Otherwise, the initial product Co_2B will be converted to cobalt metal and boron oxides under aerobic conditions as described in Equations (2) and (3) [34].

$$4Co_2B + 3O_2 \rightarrow 8Co(s) + 2B_2O_3 \quad (2)$$

$$B_2O_3 + 3H_2O \rightarrow 2B(OH)_3 \quad (3)$$

In the present work, all the CCS-supported Co catalysts were prepared under aerobic conditions. Furthermore, lots of oxygen-containing groups on the CCS support provided not only binding sites for Co^{2+} ions and the reduced Co metals, but also an oxidizing environment to promote Reaction (2). As a result, all of the as-prepared CCS-supported Co catalysts did not contain boron.

The chemical composition and phase purity of the products were determined by XRD, and the corresponding XRD patterns were shown in Fig. 3. The broad peak located at $2\theta = 20–25^\circ$ in Fig. 3 (a) is a characteristic of colloidal carbon spheres [35]. No distinct peaks were observed for the unsupported Co catalysts as shown in Fig. 3 (b), suggesting the amorphous nature of the unsupported Co catalysts. The XRD pattern of the CCS-supported Co catalysts with a Co loading of 18.38 wt% is displayed in Fig. 3 (c). The weak peak at the $2\theta = 33^\circ$ can be ascribed to Co_3O_4 due to oxidation of the cobalt metals deposited on the CCS support upon exposure to air. To investigate the effect of heat treatment on the crystallinity and the catalytic activity of the CCS-supported Co catalyst, it was further calcined under nitrogen atmosphere at 400 °C for 2 h, and the corresponding XRD pattern is depicted in Fig. 3 (d). The characteristic peaks of Co_3O_4 disappeared, while a weak peak at

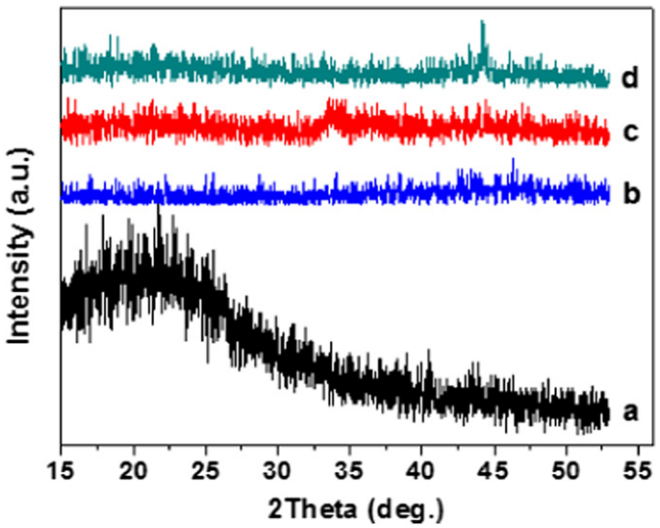

Fig. 3. XRD patterns of the CCS (a), unsupported Co catalysts (b), CCS-supported Co catalysts with a cobalt loading of 18.38 wt% before (c) and after calcination (d) under nitrogen atmospheres at 400 °C for 2 h.

$2\theta = 44^\circ$ corresponding to cobalt metal was observed. This fact indicates that the Co_3O_4 formed due to oxidation of cobalt on the surface of the CCS-support was *in-situ* reduced to cobalt metals, and aggregation/sinter of the cobalt particles might occurred simultaneously owing to the heat treatment and the loss of the oxygen-containing groups in the CCS-support.

3.2. Catalytic evaluation of the catalysts

The catalytic hydrolysis experiments were performed by dispersing 20 mg of the as-prepared materials into 10 mL of 0.2 M $NaBH_4$ solution containing 0.2 M NaOH at 20 °C. Fig. 4 shows the hydrogen generation as a function of time for four kinds of materials including colloidal carbon spheres (CCS) (a), unsupported Co particles (b), and CCS-supported Co catalysts with a Co loading of 18.38 wt% after (c) and before calcination (d). Obviously, the CCS sample had no catalytic activity towards the hydrolysis of $NaBH_4$. However, all of the Co-based materials with or without CCS-support exhibited notable catalytic activity in hydrolysis of $NaBH_4$ for hydrogen production, suggesting that the active component of the catalysts is cobalt rather than the CCS support. Furthermore, the catalytic activities of the CCS-supported Co catalysts with or without heat treatment were much better than that of the unsupported Co particles, indicating the importance of the CCS support. Similar to the function of the polymer-derived silicon carbonitride functionalized carbon nanotube paper for dispersion of a sub-nanometer layer of Co catalysts [36], the CCS support can provide a large amount of active surface to tightly anchor and uniformly disperse the chemically reduced cobalt metals, preventing aggregation of the Co particles in the process of catalyst preparation and test, and hence creating much more active catalytic sites. In contrast, aggregation of the unsupported Co particles was inevitable as shown in the lower inset of Fig. 4. Therefore, the catalytic activities of the CCS-supported Co catalysts were remarkably superior to the unsupported Co particles.

Although calcination treatment was adopted to improve the catalytic activities of some supported transition metal catalysts [37], heat treatment did deteriorate the catalytic activity of the CCS-supported Co catalysts in the present work as shown in Fig. 4 (c).

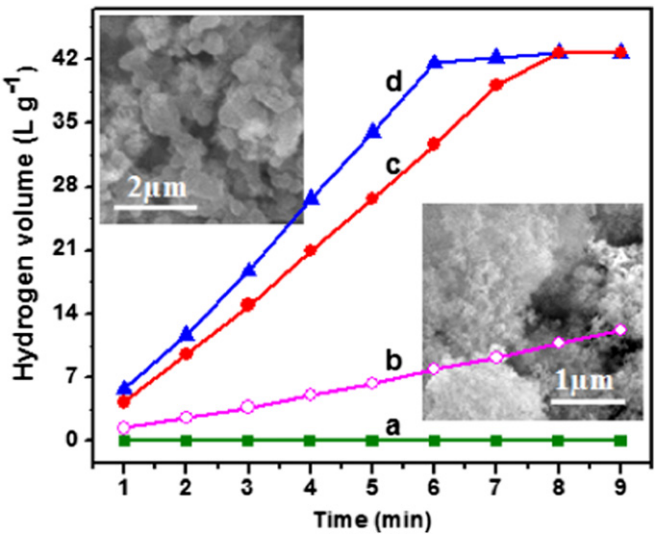

Fig. 4. Comparison of the hydrogen generation performance of different catalysts. (a) Colloidal carbon spheres (CCS); (b) Unsupported Co particles; (c) and (d) CCS-supported Co catalysts with a cobalt loading of 18.38 wt% after and before calcination, respectively. The upper and lower insets are the SEM images of the CCS-supported Co catalysts after calcination and the unsupported Co particles, respectively.

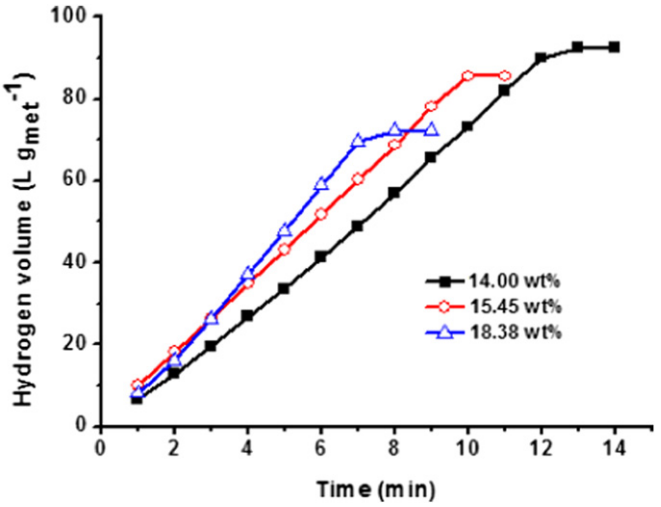

Fig. 5. Effects of the Co loading on the catalytic performance of the CCS-supported Co catalysts (20 mg) in 10 mL of 1 wt% $NaBH_4$ solution containing 10 wt% NaOH at 20 °C.

This might be caused by the loss of the surface oxygen-containing group of the CCS support, and aggregation or sinter of the Co particles as depicted in the upper inset of Fig. 4. Similar phenomena were observed for the original activated carbon (AC) and HNO_3-oxidized AC-supported Co catalysts [38]. Therefore, the as-prepared CCS-supported Co catalysts without post-calcination are the focus of the following sections.

Now that cobalt is the active component of the CCS-supported catalysts for hydrolysis of $NaBH_4$, the cobalt loading is thus an important parameter to be investigated. Fig. 5 shows the effects of the Co loading on the catalytic performance of the CCS-supported Co catalysts. The corresponding data including cobalt content, hydrogen volume (V_{H_2}), yield and hydrogen generation rate (HGR) are summarized in Table 1. It is obvious that all the CCS-supported Co catalysts exhibited excellent catalytic activity towards hydrolysis of $NaBH_4$ with the hydrogen yield over 92%, and the catalytic activity of the CCS-supported Co catalysts increased from 7.5 to 10.4 L min^{-1} g_{met}^{-1} with increase of the Co loading in the range of 14.00–18.38 wt%. When the Co loading content is 18.38 wt%, the HGR is about 8 times that of the carbon black (CB)-supported Co-B catalysts with a Co-B loading of 30 wt% [39], comparable to that of Ru/activated carbon [40]. This is reasonable, because more Co loading content creates more active sites in the CCS-supported Co catalysts when the total amount of the supported catalysts was kept the same (20 mg).

Dispersion of the active component on the support is another important parameter for consideration. For this purpose, cobalt content was fixed at 5 mg in the following experiment, while the amount of CCS support was adjusted to prepare three kinds of CCS-supported catalysts with a specific cobalt loading of 14.00 wt%, 15.45 wt%, and 18.38 wt%, respectively. Fig. 6 shows the effect of the cobalt dispersion on the catalytic performance of the CCS-supported Co catalysts. It seems that opposite results was

Table 1
Comparison of the hydrogen generation performance of the CCS-supported Co catalysts with different Co loading.

Co loading of the CCS/Co catalysts (wt%)	14.00	15.45	18.38
Cobalt content (mg)	2.8	3.1	3.7
Reaction time (min)	14	11	9
V_{H_2} (mL)	259	265	267
H_2 Yield (%)	92.6	94.8	95.5
H_2 generation rate (L min^{-1} g^{-1})	7.5	8.4	10.4

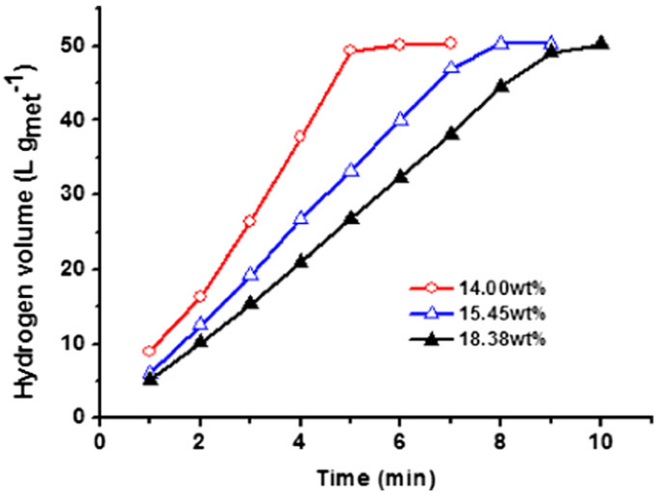

Fig. 6. Effect of the Co dispersion on the catalytic performance of the CCS-supported Co catalysts in 10 mL of 1 wt% $NaBH_4$ solution containing 10 wt% NaOH at 20 °C.

observed in comparison with the results shown in Fig. 5. Actually, it is understandable. Lower cobalt loading led to better dispersion of cobalt on the CSS support because the cobalt content was the same (5 mg) in this case. Higher dispersivity of cobalt on the hydrophilic CCS support is more propitious to reduce of aggregation of the cobalt particles, and to increase of the active sites and thus the contact between the active catalysts and the $NaBH_4$ solution, resulting in higher catalytic activity.

3.3. Effect of NaOH concentration on the hydrogen generation

As a stabilizer, NaOH is usually introduced into the $NaBH_4$ hydrolysis system to slow down the self-hydrolysis which occurs when water is added to $NaBH_4$. The influence of the NaOH concentration on the hydrogen generation was investigated and the results are demonstrated in Fig. 7. When the concentration of NaOH increased from 5 wt% to 10 wt%, the hydrogen generation was accelerated remarkably. However, when the concentration of NaOH exceeded 10 wt% the hydrogen generation rate decreased notably with increase of NaOH concentration. Probably, the OH^- ions played a dual function in the catalytic hydrolysis reaction. Low concentration of OH^- ions might increase the electrostatic repulsion among CCS-support particles (which carried with negative charges), and improve the dispersion of the CCS-supported Co catalysts in the reaction solution, and hence the contact between the catalysts and $NaBH_4$ enhanced. Therefore, the increase of OH^- concentrations from 5 wt% to 10 wt% resulted in acceleration of hydrogen generation. Whereas the inhibition of the OH^- ions for $NaBH_4$ hydrolysis would be the main function when its concentration exceeded 10 wt% [41], leading to the hydrogen generation rate decreased with increase of NaOH concentration from 15 wt% to 20 wt%. So, the optimal NaOH concentration was chosen as 10 wt% in the succedent experiments.

3.4. Effect of $NaBH_4$ concentration on the hydrogen generation

$NaBH_4$ hydrolysis reaction can be simply described as Equation (4).

$$NaBH_4 + 2H_2O \rightarrow 4H_2 + NaBO_2 + 216.7\ kJ \cdot mol^{-1} \quad (4)$$

Theoretically, higher $NaBH_4$ concentration is highly desired for achieving high hydrogen capacity, but gets restricted by the solubility limitation of $NaBH_4$ itself and hydrolysis product $NaBO_2$ in water [41]. The effect of the $NaBH_4$ concentration on the hydrogen generation is shown in Fig. 8. One can see that the concentration of $NaBH_4$ indeed exerted an important impact on the practical hydrogen generation performance in our hydrolysis system. The hydrogen generation rate evidently increased at first with increase of the $NaBH_4$ concentration from 0.5 wt% to 1wt%, and then gradually decreased with continuous increase of the $NaBH_4$ concentration in the range of 5–20 wt%, because of the solubility limitation of both $NaBH_4$ and $NaBO_2$, and an increase of the viscosity and alkalinity of the reaction mixture [42]. Therefore, the optimal $NaBH_4$ concentration was chosen as 1 wt% in the present work.

3.5. Effect of temperature on the hydrogen generation

The temperature effect on the $NaBH_4$ hydrolysis was investigated at a temperature ranging from 20 to 40 °C under the optimal

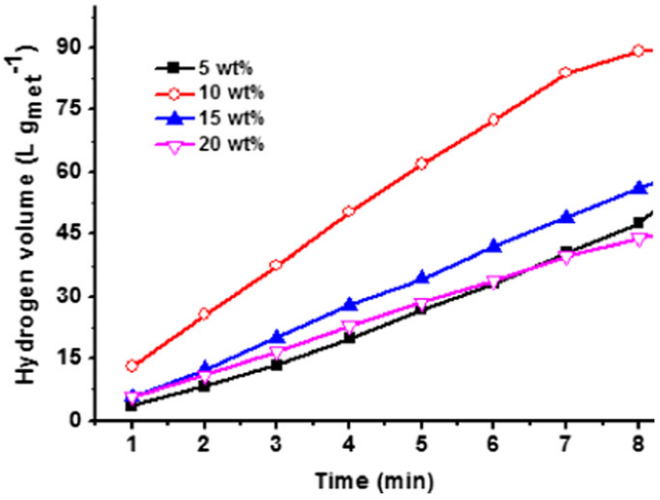

Fig. 7. Effect of the NaOH concentration on the hydrogen generation by hydrolysis of 1wt% $NaBH_4$ solution at 20 °C in the presence of 20 mg the CCS-supported Co catalysts with a cobalt loading of 18.38 wt%.

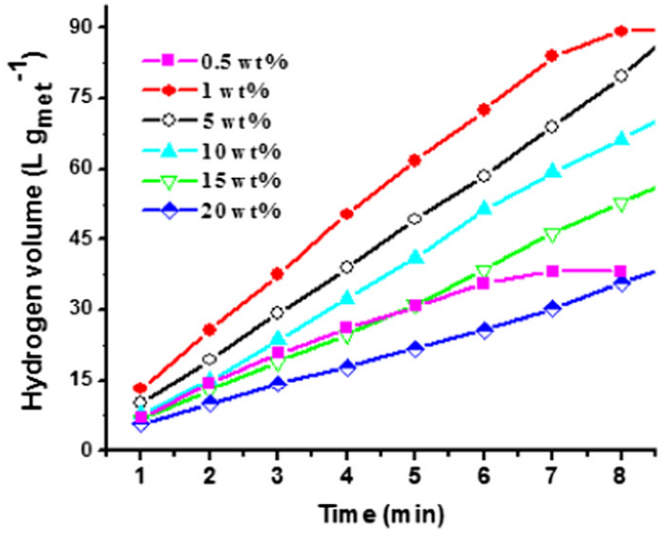

Fig. 8. Effect of the $NaBH_4$ concentration on the hydrogen generation from hydrolysis of $NaBH_4$ solution containing 10 wt% NaOH at 20 °C in the presence of 20 mg the CCS-supported Co catalysts with a cobalt loading of 18.38 wt%.

conditions: 10 mL of 1wt% $NaBH_4$ solution containing 10 wt% NaOH in the presence of 20 mg the CCS/Co catalysts with a Co loading of 18.38 wt%. From the results demonstrated in Fig. 9 one can see that hydrogen generation at any given temperature linearly increased with reaction time, indicating the zero order reaction kinetics of $NaBH_4$ hydrolysis. In addition, the initial hydrogen generation rate increased significantly with temperature. Note that no evident induction period was observed in the course of $NaBH_4$ hydrolysis catalyzed by the as-prepared CCS-supported Co catalysts at any studied temperature, indicating outstanding efficiency of the CCS-supported Co catalysts.

For comparison of catalysts activities, the initial hydrogen generation rates k (L min^{-1} g_{met}^{-1}) were derived from Fig. 9 and used to determine the activation energy by Arrhenius equation (5).

$$\ln k = \ln A - \frac{E_a}{RT} \quad (5)$$

where k is the hydrogen generation rate (L min^{-1} g_{met}^{-1}), A the pre-exponential factor, E_a the activation energy (kJ mol^{-1}), R the gas constant (8.314 J mol^{-1} K^{-1}), and T is the hydrolysis temperature (K).

The Arrhenius plot of ln k *vs.* $1/T$ is shown in Fig. 10 (a). From the slop of the straight line, the apparent activation energy for $NaBH_4$ hydrolysis was calculated to be 24.04 kJ mol^{-1}, which is much lower than the literature data as summarized in Table 2. According to Arrhenius Equation, a decrease in E_a will give rise to an exponential increase in rate k, the relatively lower activation energy (24.04 kJ mol^{-1}) in the present work indicates that the as-prepared CCS-supported Co materials are exceptionally efficient catalysts for hydrogen generation from hydrolysis of $NaBH_4$.

The data were further arranged according to Eyring equation (6) and re-plotted in Fig. 10 (b).

$$\ln\frac{k}{T} = -\frac{\Delta H^{\neq}}{R}\cdot\frac{1}{T} + \ln\frac{k_B}{h} + \frac{\Delta S^{\neq}}{R} \quad (6)$$

where k, T, and R have the same meanings as those in Equation (5). k_B is the Boltzmann constant, and h the Planck constant. $\Delta H^{\neq}$ and $\Delta S^{\neq}$ are the activation enthalpy, and entropy, respectively. Both the activation enthalpy ($\Delta H^{\neq}$) and entropy ($\Delta S^{\neq}$) of the $NaBH_4$ hydrolysis reaction can be achieved from the Eyring plot shown in Fig. 10 (b), and the corresponding value is 21.51 kJ mol^{-1} and −178.24 J mol^{-1} K^{-1}, respectively. It is worthy noting that activation entropy for the CCS-supported Co catalysts is very close to that for Co/p (AMPS) (−178.57 J mol^{-1} K^{-1}), while $\Delta H^{\neq}$ for the former (21.514 kJ mol^{-1}) is much lower than that for the later (35.46 kJ mol^{-1}) [49]. Therefore, the contribution of entropy in the two systems is almost the same, and the distinct differences in their activation energy (E_a) and enthalpy ($\Delta H^{\neq}$) values indicate that different catalytic mechanism occurred. More work is underway in our group to understand the exact catalytic mechanism in detail.

Table 2
Comparison of the effectiveness of the CCS/Co catalysts with some literature data.

Catalysts	Activation energy (kJ mol^{-1})	H_2 generation rate (L min^{-1} g_{met}^{-1})	Temperature (°C)	Ref.
Active carbon/Co	45.64	0.07	30	[43]
γ-Al_2O_3/Co	32.63	0.22	30	[43]
Vulcan XC-72/CoB	57.8	2.3	25	[39]
Al_2O_3/CoB	56.8	5.495	20	[44]
TiO_2/CoB	51.0	6.738	20	[44]
CeO_2/CoB	55.3	4.717	20	[44]
Co-Mn-B	52.1	1.44	20	[45]
Hydroxyapatite/Co	53 ± 2	5.0	25	[46]
Polycarbonate membrane/Co	54	2.64	80	[47]
Carbon/Pd	28	2.1	23	[48]
p(AMPS)/Co	38.14	0.94	30	[49]
CCS/Co	24.04	10.4	20	This work

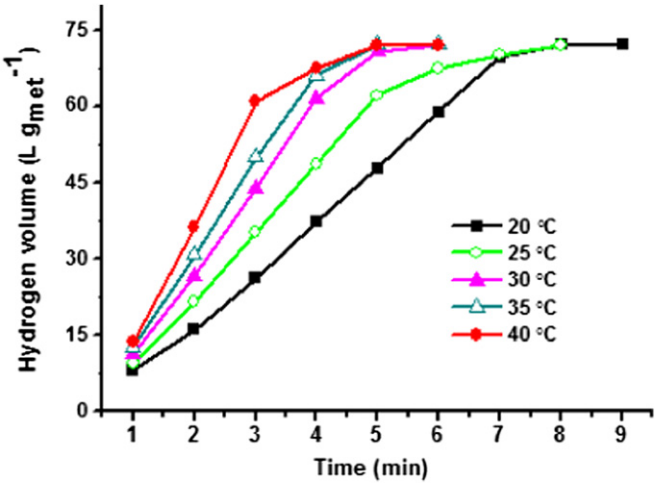

Fig. 9. Temperature effect on the hydrogen generation from hydrolysis of $NaBH_4$ solution (10 mL, 1 wt%) containing 10 wt% NaOH in the presence of 20 mg the CCS-supported Co catalysts with a cobalt loading of 18.38 wt%.

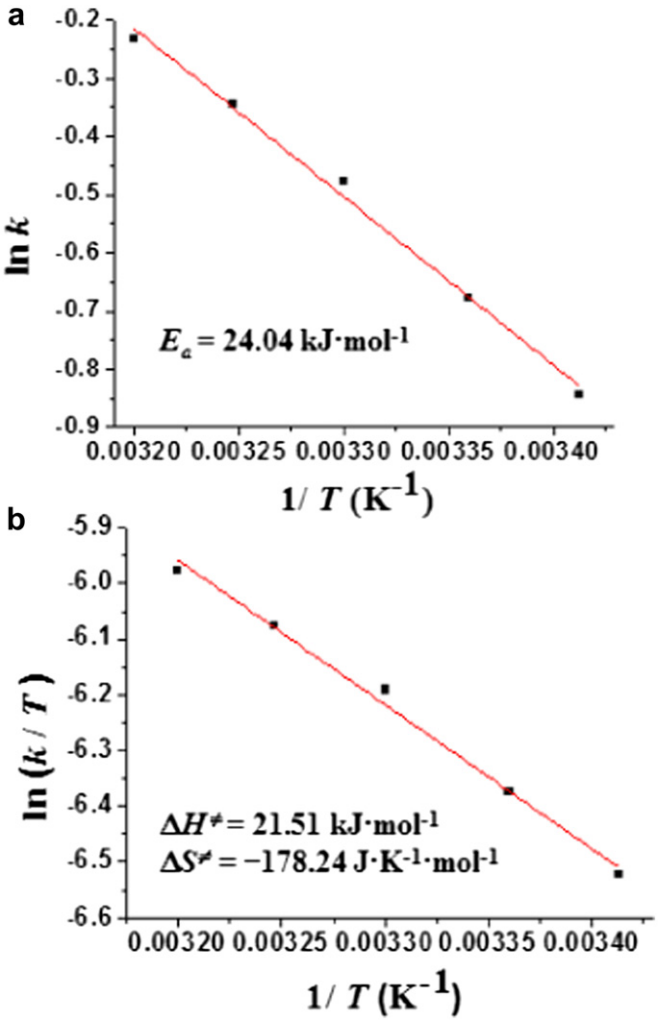

Fig. 10. (a) ln k *vs.* $1/T$ (Arrhenius plot); (b) ln (k/T) vs. $1/T$ (Eyring plot).

4. Conclusions

In summary, colloidal carbon spheres (CCS) were obtained by hydrothermal treatment of commercial glucose, and were used for the first time as the support to prepare CCS/Co catalysts with different Co loading by chemical reduction of Co^{2+} with $NaBH_4$. The morphology, composition and elemental distribution of the as-prepared CCS-supported Co catalysts were characterized by combination of SEM, XRD and EDX. Furthermore, the catalytic performances of the CCS-supported Co catalysts for hydrogen generation from hydrolysis of alkaline $NaBH_4$ solution were investigated in detail. The following conclusions can be drawn. (1) In terms of the cost, self-weight, and hydrophilic surface chemistry, the colloidal carbon spheres (CCS) act as an idea support to tightly bind Co^{2+} and the chemical reduced cobalt metals through electrostatic or coordination interactions. (2) Ultrafine and almost amorphous cobalt metals uniformly deposit on the surface of the CCS support, creating more active sites. (3) The CCS-supported Co catalysts exhibit excellent catalytic activity towards $NaBH_4$ hydrolysis thanks to their unique hydrophilic surface, which improve the contact between catalysts and $NaBH_4$ in the alkaline media. (4) The activation energy for the CCS/Co catalyzed $NaBH_4$ hydrolysis is calculated to be 24.04 kJ mol^{-1}, much lower than those for most of the previously reported catalysts including non-noble metals and precious metals with or without supports, indicating the promising applications of the CCS-supported Co catalysts for hydrogen generation or in many other fields.

Acknowledgments

This work was financially supported by the National Natural Science Foundation of China (51071131), Program for New Century Excellent Talents in University (NCET-10-0890), the Scientific Research Foundation for the Returned Overseas Chinese Scholars ([2008]488), and Chemical Synthesis and Pollution Control Key Laboratory of Sichuan Province (10CSPC-1-7).

References

[1] J.A. Turner, Science 285 (1999) 687–689.
[2] M.S. Dresselhaus, I.L. Thomas, Nature 414 (2001) 332–337.
[3] H. Marty, Nature 472 (2011) 137.
[4] N. Armaroli, V. Balzani, Angew. Chem. Int. Ed. 46 (2007) 52–66.
[5] W. Luo, P.G. Campbell, L.N. Zakharov, S.Y. Liu, J. Am. Chem. Soc. 133 (2011) 19326–19329.
[6] U. Eberle, M. Felderhoff, F. Schüth, Angew. Chem. Int. Ed. 48 (2009) 6608–6630.
[7] J. Yang, A. Sudik, C. Wolverton, D.J. Siegel, Chem. Soc. Rev. 39 (2010) 656–675.
[8] L. Schlapbach, A. Züttel, Nature 414 (2001) 353–358.
[9] B.H. Liu, Z.P. Li, J. Power Sources 187 (2009) 527–534.
[10] S. Orimo, Y. Nakamori, J.R. Eliseo, A. Züttel, C.M. Jensen, Chem. Rev. 107 (2007) 4111–4132.
[11] U.B. Deirci, P. Miele, Energy Environ. Sci. 2 (2009) 627–637.
[12] U.B. Demirci, O. Akdim, P. Miele, Int. J. Hydrogen Energy 34 (2009) 2638–2645.
[13] D.M.F. Santos, C.A.C. Sequeira, Renew. Sust. Energ. Rev. 15 (2011) 3980–4001.
[14] S.S. Muir, X. Yao, Int. J. Hydrogen Energy 36 (2011) 5983–5997.
[15] U.B. Demirci, O. Akdim, J. Andrieux, J. Hannauer, R. Chamoun, P. Miele, Fuel Cells 10 (2010) 335–350.
[16] M. Ay, A. Midilli, I. Dincer, J. Power Sources 157 (2006) 104–113.
[17] K. Kim, T. Kim, K. Lee, S. Kwon, J. Power Sources 196 (2011) 9069–9075.
[18] A.A. Vernekar, S.T. Bugde, S. Tilve, Int. J. Hydrogen Energy 37 (2012) 327–334.
[19] H. Dai, Y. Liang, P. Wang, Catal. Today 170 (2011) 27–32.
[20] Y. Kojima, K. Suzuki, K. Fukumoto, M. Sasaki, T. Yamamoto, Y. Kawai, H. Hayashi, Int. J. Hydrogen Energy 27 (2002) 1029–1034.
[21] G. Guella, C. Zanchetta, B. Patton, A. Miotello, J. Phys. Chem. B 110 (2006) 17024–17033.
[22] U.B. Demirci, P. Miele, Phys. Chem. Chem. Phys. 12 (2010) 14651–14665.
[23] V.I. Simagina, O.V. Komova, A.M. Ozerova, O.V. Netskina, G.V. Odegova, D.G. Kellerman, O.A. Bulavchenko, A.V. Ishchenko, Appl. Catal. A 394 (2011) 86–92.
[24] L. Damjanović, M. Majchrzak, S. Bennici, A. Auroux, Int. J. Hydrogen Energy 36 (2011) 1991–1997.
[25] H. Tian, Q. Guo, D. Xu, J. Power Sources 195 (2010) 2136–2142.
[26] S. Bennici, H. Yu, E. Obeid, A. Auroux, Int. J. Hydrogen Energy 36 (2011) 7431–7442.
[27] N. Sahiner, O. Ozay, E. Inger, N. Aktas, J. Power Sources 196 (2011) 10105–10111.
[28] Z. Liu, B. Guo, S.H. Chan, E. Tang, L. Hong, J. Power Sources 176 (2008) 306–311.
[29] H. Dai, Y. Liang, P. Wang, H. Cheng, J. Power Sources 177 (2008) 17–23.
[30] N. Patel, R. Fernandes, N. Bazzanella, A. Miotello, Catal. Today 170 (2011) 20–26.
[31] C. Yang, M. Chen, Y. Chen, Int. J. Hydrogen Energy 36 (2011) 1418–1423.
[32] X. Sun, Y. Li, Angew. Chem. Int. Ed. 43 (2004) 597–601.
[33] G.M. Arzac, T.C. Rojas, A. Fernández, ChemCatChem 3 (2011) 1305–1313.
[34] G.N. Glavee, K.J. Klabunde, C.M. Sorensen, G.C. Hadjapanayis, Langmuir 8 (1992) 771–773.
[35] X. Lai, J. Li, B.A. Korgel, Z. Dong, Z. Li, F. Su, J. Du, D. Wang, Angew. Chem. Int. Ed. 50 (2011) 2738–27411.
[36] L. Hu, R. Ceccato, R. Raj, J. Power Sources 196 (2011) 69–75.
[37] D. Xu, P. Dai, X. Liu, C. Cao, Q. Guo, J. Power Sources 182 (2008) 616–620.
[38] D. Xu, P. Dai, Q. Guo, X. Yue, Int. J. Hydrogen Energy 33 (2008) 7371–7377.
[39] J. Zhao, H. Ma, J. Chen, Int. J. Hydrogen Energy 32 (2007) 4711–4716.
[40] C. Crisafulli, S. Scirè, M. Salanitri, R. Zito, S. Calamia, Int. J. Hydrogen Energy 36 (2011) 3817–3826.
[41] Y. Liang, H. Dai, L. Ma, P. Wang, H. Cheng, Int. J. Hydrogen Energy 35 (2010) 3023–3028.
[42] S.U. Jeon, R.K. Kim, E.A. Cho, H.J. Kim, S.W. Nam, I.H. Oh, S.A. Hong, S.H. Kim, J. Power Sources 144 (2005) 129–134.
[43] W. Ye, H. Zhang, D. Xu, L. Ma, B. Yi, J. Power Sources 164 (2007) 544–548.
[44] Y. Lu, M. Chen, Y. Chen, Int. J. Hydrogen Energy 37 (2012) 4254–4258.
[45] X. Yuan, C. Jia, X. Ding, Z. Ma, Int. J. Hydrogen Energy 37 (2012) 995–1001.
[46] M. Rakap, S. Özkar, Catal. Today 183 (2012) 17–25.
[47] O. Akdim, R. Chamoun, U.B. Demirci, Y. Zaatar, A. Khoury, P. Miele, Int. J. Hydrogen Energy 36 (2011) 14527–14533.
[48] N. Patel, B. Patton, C. Zanchetta, R. Fernandes, G. Guella, A. Kale, A. Miotello, Int. J. Hydrogen Energy 33 (2008) 287–292.
[49] N. Sahiner, O. Ozay, E. Inger, N. Akas, Appl. Catal. B 102 (2011) 201–206.